Tellus
SERIES A DYNAMIC METEOROLOGY AND OCEANOGRAPHY
PUBLISHED BY THE INTERNATIONAL METEOROLOGICAL INSTITUTE IN STOCKHOLM

Tellus (2009), 61A, 154–159
Printed in Singapore. All rights reserved

TELLUS

Impact of tropospheric and stratospheric data assimilation on mesospheric prediction

By YULIA NEZLIN[1]*, YVES J. ROCHON[2] and SAROJA POLAVARAPU[2], [1]*Department of Physics, University of Toronto, 60 St. George Street, Toronto, Ontario, Canada;* [2]*Atmospheric Science and Technology Directorate, Environment Canada, Toronto, Ontario, Canada*

(Manuscript received 9 April 2008; in final form 10 September 2008)

ABSTRACT

Numerical experiments are used to assess the potential benefit of the assimilation of tropospheric and stratospheric observations on mesospheric prediction. A simulated atmosphere, taken as truth, is created using the Canadian Middle Atmosphere Model (CMAM). The truth is sampled at the locations of the measurements from the actual observing system to produce observations, which are then assimilated with the CMAM-DAS (Data Assimilation System). Obtained forecasts are compared with the truth, and error statistics are calculated. An assessment based on predictability shows that upward propagation of information resulting from the assimilation of tropospheric and stratospheric observations improves the mesosphere in the largest scales (with horizontal wavenumbers less than approximately 10). At the same time, the principal inability of the system to predict mesospheric small scales is demonstrated.

1. Introduction

The departure of the middle atmosphere from radiative equilibrium is mainly due to dynamic forcing by waves that propagate up from the troposphere (Andrews et al., 1987). Because waves (and thus information) propagate upwards, tropospheric and stratospheric observations contain information about the mesosphere and mesospheric forecasts should be able to benefit from their assimilation. On the other hand, assimilation generates noise or spurious waves that grow to large amplitudes in the mesosphere (Sankey et al., 2007). As a result, mesospheric analyses and forecasts strongly depend on the ability of an assimilation system to control the growth of spurious waves. In Sankey et al. (2007), the sensitivity of mesospheric analyses to a filtering procedure applied to suppress the spurious waves generated in the troposphere and stratosphere was analysed. It was shown that basic features of the mesospheric flow such as tides may be easily lost by 'over-filtering' or 'under-filtering'. The present work quantifies the effect of tropospheric and stratospheric observations on the mesosphere with the Canadian Middle Atmosphere Model-Data Assimilation System (CMAM-DAS). Observations derived from a simulated atmosphere taken as truth are assimilated and the resulting analyses and forecasts are evaluated against this same truth. The resulting differences are compared with predictability errors (defined below) obtained without observational information to demonstrate the benefit of tropospheric and stratospheric observations in propagating information to the mesosphere through the numerical prediction model. This comparison shows that the positive impact in correctly resolving features of the mesosphere is scale-dependent. The scales over which this impact is achieved are identified.

*Corresponding author.
e-mail: yulia.nezlin@ec.gc.ca
DOI: 10.1111/j.1600-0870.2008.00368.x

2. Short description of the data assimilation system

We use the CMAM model at a T47 resolution and with a lid at about 95 km. The CMAM is a complex General Circulation Model with interactive chemistry, radiation and dynamics (Beagley et al., 1997; de Grandpré et al., 2000). McLandress et al. (1997), Manson et al. (2002) and Sica et al. (2007) have shown that the CMAM has a realistic amount of mesospheric variability, by comparing against mesospheric observations.

An Incremental Analysis Updating scheme (IAU), as first proposed in Bloom et al. (1996), is used to suppress the growth of spurious waves. The benefit of this filter and its comparison with the other existing filtering schemes was investigated in Sankey et al. (2007) in the context of mesospheric dynamics.

A 3-D variational assimilation scheme is used to assimilate observations from surface stations, radiosondes, aircrafts, cloud-drift winds and AMSU-A brightness temperatures for channels 5–13 from NOAA-15 and NOAA-16 satellites (Polavarapu et al., 2005). An assimilation cycle proceeds as follows.

Observations from a 6-h window are assimilated and an estimation of the atmospheric state (called an 'analysis') is produced. Then, the model integration starting from the analysis is performed to produce a prediction for the next synoptic time (called the 6-h forecast) when the next set of observations will be assimilated. Currently, we do not assimilate observations higher than 1 hPa (about 50 km), and there are no vertical correlations propagating information above this level, so, analysis increments are negligible in that region. Thus observations can only influence the mesosphere through the model integration during 6-h forecasts and not during the analysis step.

3. Description of the experiments

First, a free model run (without data assimilation) is started from an analysis to generate a reference simulation, which is taken as the truth. 'Perfect' observations are created by sampling the truth at the locations of the measurements from the actual observation data set described in the previous section. The observation simulations are performed using the observation forward models of the assimilation system. The simulated observation data set is produced by replacing the values of the actual observations with those of the background state in observation space. This is done during a 3D-Var cycle for the reference simulation in which observations were read in but were not assimilated. The saved simulated observations are then perfectly consistent with the reference model simulation, and they reflect actual observed variables, such as brightness temperatures.[1] The resultant data set is consistent with the density and types of measurements of the actual observation network. Although our system uses fewer measurements than an operational system, the type and distribution of measurements is representative of operational systems. Random errors may be added to the 'perfect' observations to simulate observational errors. These errors satisfy a Gaussian distribution with zero mean and covariances given by the specified observation error covariance matrix. Thus created, perfect and perturbed observation sets are then separately assimilated in two data assimilation (DA) cycles. The 6-h forecast and analysis errors calculated in model grid space are differences between the 6-h forecasts and analyses taken from the assimilation cycles and the 'truth' generated by the reference simulation. These errors are sampled every 6 h, over a one-month period.

The global 6-h forecast (and analysis) error standard deviations grow during the first two weeks until they reach nearly stationary values. Therefore, only the last 10 d of the month are used to estimate the latitudinally varying stationary part of forecast error levels (It was verified that the statistical results do not change when a longer period of 20 d is used. Periods longer than one month are not desirable because of seasonal effects). An ensemble set of 10 d provides 40 error samples per grid point in the calculation of error variances. With the additional zonal averaging of error variances, the number of error samples is multiplied by the number of longitudes and is thus 40×96.

Although analysis errors in observation space are smaller than forecast errors, at locations of model gridpoints, they are found to be nearly the same. The explanation of this is different for different regions. In the mesosphere the analysis exactly coincides with background since there are no observations and analysis increments are forced to zero. A significant part of the troposphere is data sparse (e.g. the oceans) and is not affected by the majority of highly accurate radiosonde observations. In the stratosphere, where observations are mainly of radiances, which are related to column integrals of temperature, the errors are significantly increased when they are projected onto model space and the difference between analysis and forecast error becomes negligible. Thus, the results provided below, referring to 6-h forecast error levels on the model grid, can be taken as also representative of analysis error levels.

By using the same model in producing the simulated observations and the forecasts used in assimilation, we implicitly assume that the model is 'perfect' (i.e. the model is consistent with the reality reflected by observations).

3.1. Best case scenario

In the 'best case' scenario, perfect observations are assimilated and the assimilation starts from perfect initial conditions (i.e. taken from the truth). Therefore, one might expect that the errors would have been zero in this experiment. However, this is not the case as seen in Fig. 1a, where the standard deviations of 6-h forecast errors for January temperatures are shown for the 'best case' scenario. Figure 1a shows that the error levels are relatively small in the troposphere (with a maximum in the tropics) but increase with height, attaining values of 20 K in the mesosphere, with values being almost $2^{1/2}$ larger than the standard deviation of climatological variability computed as monthly mean standard deviation of the atmosphere from its monthly average over 20 yr (not shown). This size difference with climatological variability is discussed later.

During the very first analysis step, numerical precision errors result in small analysis increments. These are initially localized in the vicinity of observations, that is, in the troposphere and stratosphere. The small analysis errors are gradually amplified and spread by the forecast model, ultimately reaching regions far from the observations, including the mesosphere. Over successive analyses, the observations restrain the forecast errors but errors grow again during the subsequent forecast. Forecast error levels saturate within two weeks at the values shown in Figure 1a, which then become stationary. It would appear that resultant error levels in the mesosphere are dictated by

[1]Because 3D-Var was used, the background state is valid at the analysis time; so, observations are simulated exactly at the analysis time. The analysis and forecast errors therefore do not include errors due to temporal displacement of observations and the background state.

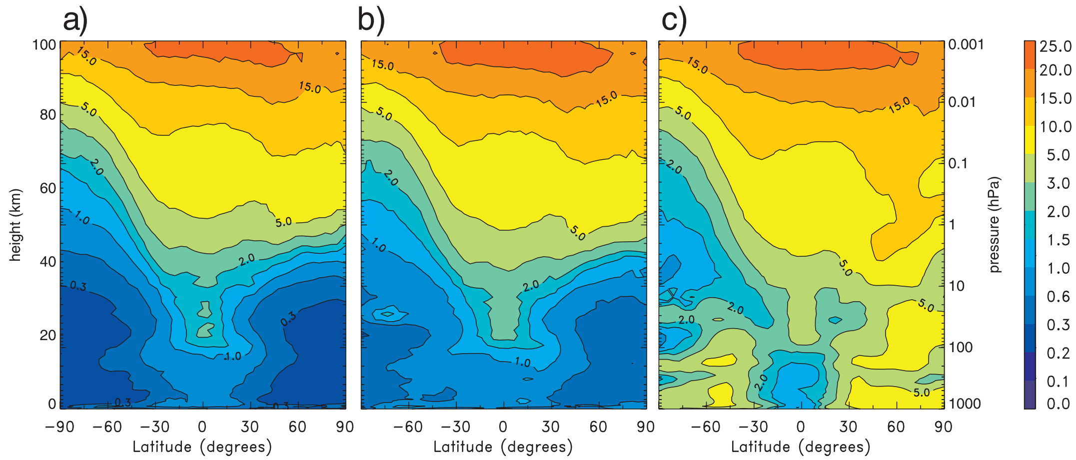

Fig. 1. Zonally averaged January temperature error standard deviations in Kelvin for 6-h forecast errors for (a) the 'best case' scenario (with assimilation of perfect observations) and (b) the case with perturbed observations and perturbed initial conditions. (c) The CMAM predictability errors (with no assimilation).

climatological variability, whereas in data dense regions, the error growth is controlled by the observations and is actually halted at levels far below the climatological variability.

Clearly, in an assimilation cycle with real (not simulated) measurements, the errors of 6-h forecasts can only be larger. Therefore, Fig. 1a shows the minimum error level that appears in a system with perfect observations and a perfect model. This minimum error level demonstrates the ability of an assimilation system to control the growth of instabilities that are present in the forecasts.

3.2. *More realistic scenario*

For a more realistic scenario, random errors are added to the originally noise-free observations. As well, error is imposed on the initial conditions by taking a state from the truth for the same synoptic time but valid 3 d later. The errors of the initial conditions are rather large (with overall sizes close to the standard deviations of climatological variability) but not so large as to result in a model failure during the assimilation cycle.

The initially large 6-h forecast error levels rapidly decrease and saturate to stationary values at the levels shown in Fig. 1b after about two weeks. As seen by comparing with Fig. 1a, the minimum 6-h forecast error levels are roughly doubled in the troposphere, but are almost unaffected in the mesosphere (most certainly, because it is already close to the maximum dictated by climatological variability).

3.3. *Scenario without data assimilation*

Since the variances of 6-h forecast errors in the mesosphere are almost twice those from climatological variability, it might seem that there is ultimately no geophysically meaningful information propagated upwards to the mesosphere during an assimilation cycle. A 1-month simulation without data assimilation was conducted to determine whether or not this is in fact the case. It is used for comparison in the spectral analyses of Sections 4 and 5. For this simulation, the model forecast errors relative to our 'truth' result only from errors (differences) in the initial conditions. The first analysis obtained from the ideal scenario case (valid 6 h after the simulation start) was applied as initial state. Error standard deviations are calculated from the differences taken at 6-h intervals between this 1-month simulation and the truth. These standard deviations increase with time during the first two weeks after which they become stationary, as did the standard deviations of 6-h forecast errors from the assimilation cycles. This stationary level does not depend on initial conditions chosen in the simulation but is defined by the model climatological variability. These error levels are shown in Fig. 1c and reflect the sensitivity of the CMAM forecasts to errors in initial conditions. This sensitivity is often called the predictability error (Lorenz, 1965; Daley, 1991). This error is related to the non-linearity of the model and becomes rather significant in the mesosphere. The differences taken at 6-h intervals between this 1-month simulation and the truth are therefore referred to as predictability errors in this paper.

A comparison with Fig. 1a reveals that assimilation significantly reduces the predictability error levels in the troposphere (which is what we expect when assimilating observations in this region), whereas in the mesosphere, the 6-h forecast error levels from the DA cycle are nearly the same as the predictability error levels (without DA). As such, only comparing error standard deviations does not reveal any significant difference between these cases in terms of impact from upward propagation of information on the mesosphere.

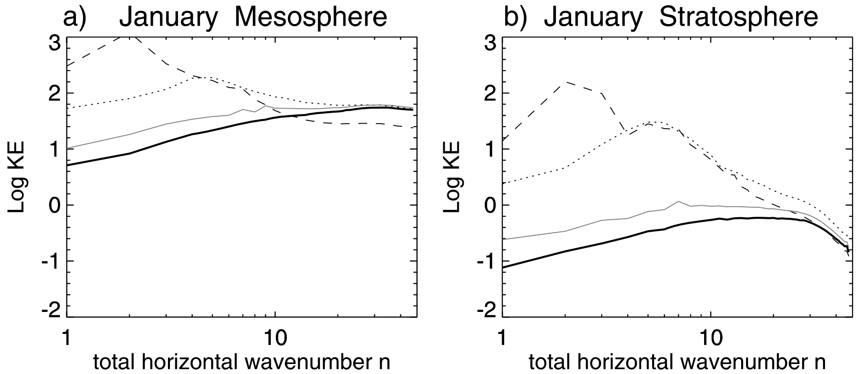

Fig. 2. Log_{10} of kinetic energy spectra in J kg^{-1}, averaged vertically and in time. The solid lines present the 6-h forecast errors from the CMAM-DAS with perfect observations (black) and with perturbed observations (grey). Dotted lines refer to the predictability errors of the CMAM. Dashed lines are from the full states of the CMAM (computed from a reference simulation). The vertical averages are taken over the following vertical ranges: stratosphere, 110–1 hPa (∼15–50 km); mesosphere, 1–0.001 hPa (∼50–95 km). Time averaging is done over 10 d.

4. Error spectra

The forecast errors in Fig. 1 involve contributions from all spatial scales. In this section, we examine the energy distribution of the forecast errors as a function of horizontal wavenumber. The kinetic energy spectra are calculated using an expansion in a series of spherical harmonics as in Boer (1983). Figure 2 shows kinetic energy spectra in total horizontal wavenumbers averaged over the mesospheric (1–0.001 hPa) and stratospheric layers (110–1 hPa). The spectra were also averaged over 10 d (40 samples). The solid black lines depict the 6-h forecast error spectra for the 'best case' scenario.

As seen in Fig. 2a, the energy of the 6-h forecast errors grows with increasing wavenumber in the mesosphere. In fact, there is more than double the energy at small scales than at large scales. Therefore, the largest errors in the mesosphere are at small scales. For comparison, the spectra of the full field (not of the errors) are shown in the figure by the dashed lines. At large scales, the energy of forecast errors is smaller than that of the full field, whereas at small scales, the energy of forecast errors is twice as large as that of the field itself. This is possible if small-scale waves (in the assimilation cycle and in the reference model run) are statistically independent, so as to give variances of their differences that are twice the variances of either state. This also explains the differences in mesospheric standard deviations between forecast errors and climatological variability noted in the discussion of Fig. 1. It is useful to compare the 6-h forecast error energy spectrum with the energy spectrum for the longer-term predictability error (dotted curve), as it provides a lower limit on forecast quality. The energy from predictability errors (dotted curve) is larger than that for the full state for small scales but is smaller for large scales. In the mesosphere, the energy of 6-h forecast errors for large scales is still much smaller than that of predictability errors, whereas they are the same for small scales.

At the point where the solid and dashed curves intersect ($n \sim 10$), the energy of the errors equals the energy of the state itself. Thus, only large-scale mesospheric features characterized by wavenumbers smaller than about 10 can be resolved from observation information assimilated at lower levels and propagated upwards by the model. So, wavenumber 10 approximately separates predictable and unpredictable mesospheric scales, when only observations from below the mesosphere are assimilated.

Note that at wavenumber 10, the divergent and rotational components of kinetic energy in the mesosphere become comparable and for larger wavenumbers the flow is mostly unbalanced (Koshyk et al., 1999). For large scales ($n < 10$), the mesospheric flow is balanced and is controlled by the tropospheric and stratospheric dynamics. Therefore, it is reasonable to expect that these waves will be predictable with only tropospheric and stratospheric observations. Mesospheric small-scale waves can also originate locally, and their forecast, in such case, cannot be improved without mesospheric observations.

A solid grey line depicts the 6-h forecast error energy spectra for the assimilation with 'perturbed' observations. In this case, the 6-h forecast error energy is higher than in the case with perfect observations. Thus, the mesospheric forecasts benefit from the accuracy of tropospheric and stratospheric observations. Moreover, mesospheric large scales are still predictable with observations that are not perfect.

In the stratosphere, the balanced flow is limited by wavenumbers around 20 (Koshyk et al., 1999), and correspondingly, the range of predictable scales in Fig. 2b is wider than in Fig. 2a. Even unbalanced (smaller) scales (up to $n \sim 30$) are predictable in the stratosphere with an assimilation of perfect observations. The predictability of small stratospheric scales is still limited since these scales are not well observed. With perturbed observations, predictable stratospheric scales are restricted to wavenumbers within about 20 (Fig. 2b). However, in the stratosphere, the

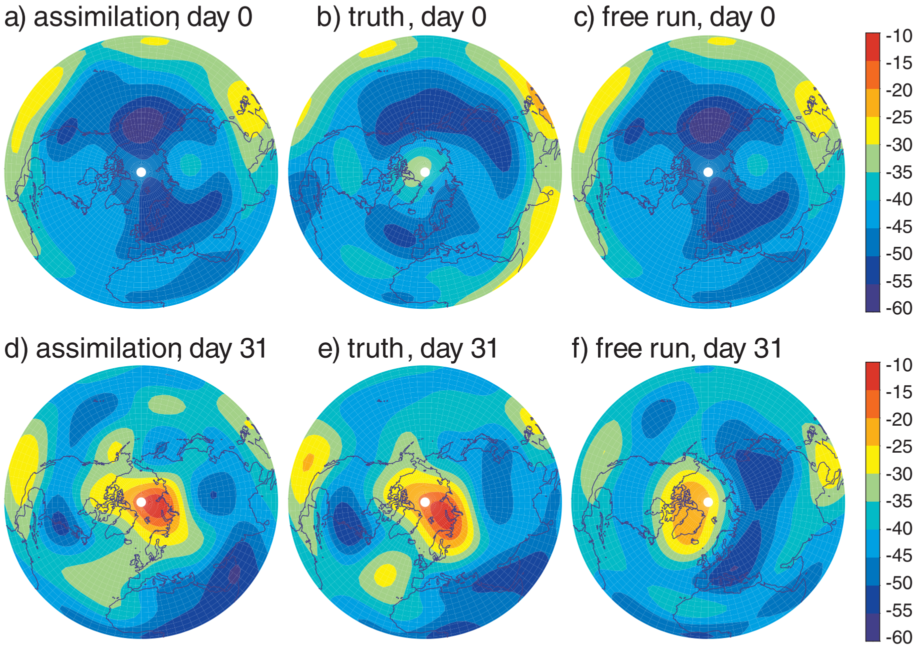

Fig. 3. Temperature fields truncated at wavenumber 10 at 0.125 hPa (∼65 km). The first row of panels represents the initial states for 1 January 2002, 00 UT for (a) the assimilation, (b) the reference or truth and (c) the second free model run without assimilation. The bottom row of panels shows temperature forecasts of large scales for 31 January 2002, 00 UT from (d) the assimilation, (e) the truth and (f) the second free model run.

relative power of the errors at small scales is much less than in the mesosphere, so, their 'predictability' is less important.

In the lower troposphere, all the scales (at least to T47) are predictable (not shown).

In summary, results in this section indicate that large scales, associated with balanced flow, are resolvable in general through data assimilation. This applies even when information from observations only originates from other regions, as is the case for the mesosphere. On the other hand, small scales, associated with unbalanced flow, are not as easily or likely resolvable even with in situ observations.

5. Prediction of mesospheric polar temperatures

The benefit of using tropospheric and stratospheric observations on mesospheric forecasts may be illustrated by comparing forecasts and true fields. Figure 3 shows temperature fields at 0.125 hPa (about 65 km) truncated at wavenumber 10. The assimilation started on 1 January 1 2002, 00 UTC from an initial state of the atmosphere that is notably different from the truth (Figs. 3a and b). Perturbed observations were assimilated in this experiment to simulate a real assimilation process. The initial condition for the assimilation was taken from the truth for the same synoptic time but 2 d later (on 3 January 2002, 00 UTC). However, after a month of assimilation, the forecast of large scales is quite close to the truth (Figs. 3d and e). The free model run (without DA) started from the same initial condition as the assimilation cycle but results in a completely different structure (Figs. 3c and g).

This example illustrates that upward propagation of information from tropospheric and stratospheric measurements results in correctly resolved large-scale mesospheric features.

6. Summary

We have quantified the impact of tropospheric and stratospheric observations on mesospheric forecasts and showed that, in spite of the inevitable noise accompanying the data assimilation process, information from below still reaches the mesosphere and makes large mesospheric scales predictable. The results imply that DA systems with models that incorporate most or all of the mesosphere but do not assimilate mesospheric data, may still result in improved mesospheric analyses on large scales (wavenumbers smaller than 10). Moreover, comparison of mesospheric analyses from such systems against measurements should be restricted to large scales.

The CMAM model used in our simulations allows more variability than many other models (Koshyk, 1999), which makes it more difficult to control the error growth in a data assimilation cycle. Nevertheless, the applied assimilation method is shown to be capable of controlling large scales with this model.

One can expect that the ability to control large mesospheric scales will also be possible with other models, since the propagation of information at large scales from the troposphere, up to the mesosphere is described by the same physics in other models.

On the other hand, we showed the inability of the CMAM-DAS (even with a perfect model) to predict small-scale events in the mesosphere and the upper stratosphere. This sets scale-dependent limits on mesospheric predictability from assimilation with the current operational observation network.

Ultimately, one hope of using data assimilation with a climate model is to use measurements to constrain aspects of model dynamics such as the parameters used in gravity wave drag schemes. Here, we show that mesospheric analyses may be useful for such studies, at least on the largest scales. Furthermore, only the largest scales in mesospheric observations may be related to parameters used to define gravity wave sources (since the sources are in the troposphere). The remaining scales might only contribute to noise in retrieved parameters.

7. Acknowledgments

This research has been supported by the C-SPARC Network, with funding from the Canadian Foundation for Climate and Atmospheric Sciences and the Canadian Space Agency and in-kind support from Environment Canada. The authors thank Ted Shepherd and Charles McLandress for many useful insights that have helped improve the paper.

References

Andrews, D. G., Holton, J. R. and Leovy, C. B. 1987. *Middle Atmosphere Dynamics*, Academic Press, San Diego, CA.

Beagley, S. R., de Grandpre, J., Koshyk, J. N., McFarlane, N. A. and Shepherd, T. G. 1997. Radiative-dynamical climatology of the first-generation Canadian Middle Atmosphere Model. *Atmos.-Ocean* **35**, 293–331.

Bloom, S. C., Takacs, L. L., da Silva, L. L. and Ledvina, D. 1996. Data assimilation using incremental Analysis Updates. *Mon. Wea. Rev.* **124**, 1256–1271.

Boer, G. J. 1983. Homogeneneous and isotropic turbulence on the sphere. *J. Atmos. Sci.* **40**, 154–164.

Daley, R. 1991. *Atmospheric Data Analysis*, Cambridge University Press, Cambridge.

de Grandpré, J., Beagley, S., Fomichev, V., Griffioen, E., M^cConnell, J. and co-authors. 2000. Ozone climatology using interactive chemistry: Results from the Canadian Middle Atmosphere Model. *J. Geophys. Res.* **105**(D21), 26 475–26 491.

Koshyk, J. N., Boville, B. A., Hamilton, K., Manzini, E. and Shibata, K. 1999. Kinetic energy spectrum of horizontal motions in middle-atmosphere models. *J. Geophys. Res.* **104**, 27 177–27 190.

Lorenz, E. N. 1965. A study of the predictability of a 28-variable atmospheric model. Tellus **17**, 321–333.

McLandress, C. 1997. Seasonal variability of the diurnal tide: Results from the Canadian middle atmosphere general circulation model. *J. Geophys. Res.* 102(D25), 29 747–29 764.

Manson, A. H., Meek, C. E., Hagan, M., Koshyk, J., Franke, S., and co-authors. 2002. Seasonal variations of the semi-diurnal and diurnal tides in the MLT: multi-year MF radar observations from 2–70°, modelled tides (GSWM, CMAM). *Ann. Geophys*. **20**, 661–677.

Polavarapu, S., Ren, S., Rochon, Y., Sankey, D., Ek, N., and co-authors. 2005. Data assimilation with the Canadian Middle Atmosphere Model. *Atmos.-Ocean* **43**, 77–100.

Sankey, D., Ren, S., Polavarapu, S., Rochon, Y., Nezlin, Y., and co-authors. 2007. The impact of data assimilation filtering methods on the mesosphere. *J. Geophys. Res.* **112**, D24104, doi:10.1029/2007JD008885.

Sica, R. J., Argal, P. S., Shepherd, T. G. and Koshyk, J. N. 2007. Model-measurement comparison of mesospheric temperature inversions, and a simple theory for their occurrence. *Geophys. Res. Lett.* **34**, L23806.